

# Fabrication of CPP devices using Chemical Mechanical Planarization

Miguel Filipe da Cunha Martins Pratas Leitão

*Under supervision of Dr Susana Isabel Pinheiro Cardoso de Freitas*

*Instituto de Engenharia de Sistemas e Computadores, Microsistemas e Nanotecnologias*

*Universidade Técnica de Lisboa, Lisbon, Portugal*

May 18, 2013

## Abstract

The work in this thesis shows the fabrication of Current Perpendicular to Plane (CPP) magnetoresistive sensors using CMP, and the use of this technique to reduce undesired topography. MTJs have been used for read heads and MRAM. Nano-oscillators based on MTJs are also an application for this type of sensors. To fabricate nano-oscillators, the MTJ pillar's area needs to be very small (smaller than 100nm), which makes it extremely difficult to do using the standard lift-off based process. Chemical mechanical planarization presents an alternative to this process. Micrometer size sensors fabricated using this techniques are demonstrated to have a MR response, with TMR values between 28,88% and 113,21%. The reduction of undesired topography has also been demonstrated.

**Keywords:** Magnetoresistive Sensors, Magnetic Tunnel Junctions, Chemical Mechanical Polishing.

## 1 Introduction

Magnetic Tunnel Junctions (MTJ) have begun to be increasingly used in commercial applications, from read heads of hard drives for computers, to RAM memory circuits. Other applications for which the magnetic tunnel junctions are beginning to be profiled is the use as high frequency oscillators. For these applications to be achieved,

the cross-sectional area of the pillars that constitute the active part of the sensor has to reduce their dimensions to below sub-100nm. For this, the method used until now (lift-off) is very slow and a new technique is used: chemical-mechanical polishing (CMP). This work aimed to study the fabrication of magnetic tunnel junction sensors, using CMP to open contact with the pillars after electri-

cally insulated with silicon dioxide.

Another objective studied in this work is the elimination of undesired topography that appears during the fabrication process. Some of the processes used to microfabricate sensors can leave undesired topography that can interrupt the levels above; this can open a contact between two metallic levels that are supposed to be insulated or interrupt a metallic line/contact between two points. This work aimed also at the reduction of this undesired topography.

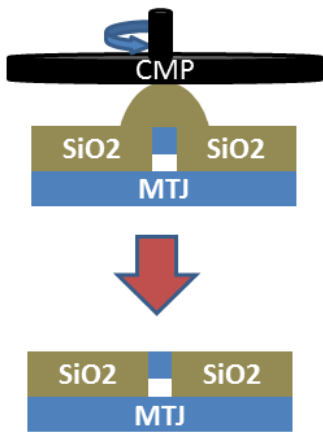


Figure 1: CMP use to open contact with the pillar through the oxide.

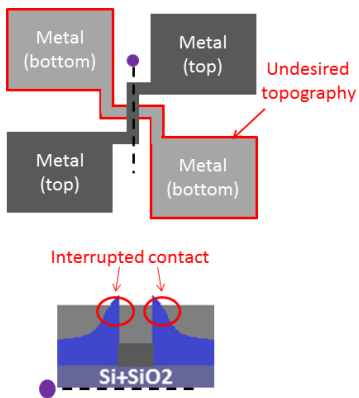


Figure 2: Possible problem for a lift-off process.

## 2 Microfabrication

To study the two objectives, two very similar processes were used to manufacture similar samples. The layers of the MTJ structure were deposited at INL by sputtering using the Timaris Singulus tool.

### 2.1 Pillar access

For the pillar access by CMP, the stack TJ417 was used (Si / SiO<sub>2</sub> 100 / Ta 5 / Ru 15 / Ta 5 / Ru 15 / Ta 5 / Ru 15 / PtMn 17 / CoFe<sub>30</sub> 2 / Ru 0,85 / CoFe<sub>30</sub> 2 / Ru 0,85 / CoFe<sub>40B20</sub> 2,6 / MgO 1 / CoFe<sub>40B20</sub> 3 / Ta 0,21 / NiFe 8 / IrMn 8 / Ru 2 / Ta 5 / Ru 10 / Ta 30); bulk material proprieties were characterized upon annealing for 2h at 330°C using a CIPT Capres tool prior to microfabrication.

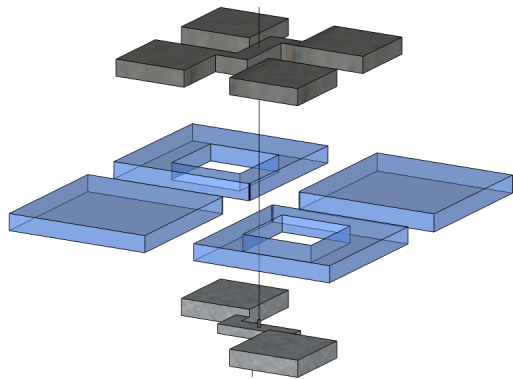


Figure 3: Sensor design, exploded view.

The microfabrication process consists in a lithography step to pattern, followed by ion milling to define the bottom contact; a second lithography to pattern, followed by another ion milling step to define the MTJ pillar and contacts. Photoresist was then removed and 300nm of SiO<sub>2</sub> were deposited by sputtering using Alcatel sputtering

system to insulate the pillar and force the current to tunnel through the barrier. Structures in the sample were measured using the profilometer, in heights A-B, A-C and A-D, for each structure (fig. 4).

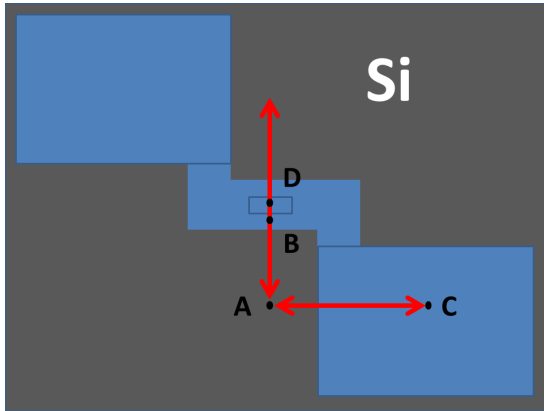


Figure 4: Relative heights measured in each sensor.

The sample was then polished using CMP, to open contact with the pillar's top, and measured again using the profilometer. The optical microscope was used to verify which sensors at each polishing step weren't covered in oxide, and confirmed with an electrical measurement. If the contact pad presented signs of not having oxide on top (fig. 5) and the resistance presented was finite, the sensor was assumed to be ready to continue with the microfabrication process. A third lithography was then performed to pattern the top contact and metallization of 300nm of AlSiCu were deposited by sputtering and defined by lift-off.

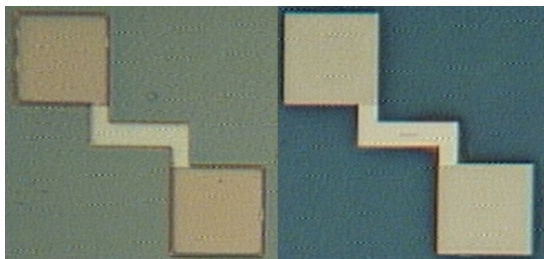


Figure 5: Contact pads (microscope). Left: covered in oxide; right: contact pad without oxide.

## 2.2 Lift-off ears

For the lift-off ears reduction, the stack TJ62: Si / SiO<sub>2</sub> 100 / Ta 5 / CuN 50 / Ta 3 / Ru 5 / IrMn 7,5 / CoFe30 2 / Ru 0,85 / CoFe40B20 2,5 / Mg 1 / NOX 1,5 / Mg 0,3 / CoFe40B20 2,5 / Ta 10 / CuN 30 / Ru 7 / TiW 50 was used (values in nm). The microfabrication process was similar to the first one: a first lithography followed by etch to define the bottom electrode. After this, 300nm of SiO<sub>2</sub> were deposited and the photoresist beneath the oxide was removed by lift-off. Several structures were measured on each sample using a profilometer. The samples were then polished using CMP and measured again to verify the ears height. This process (profilometer, CMP, profilometer) was repeated until the heights 'a' (fig.6) measured with the profilometer were (practically) 0nm.



Figure 6: The measured height, 'a'.

### 3 Results

#### 3.1 Ears planarization

The reduction of lift-off ears using CMP can be observed in fig.9. After 2 minutes, using the conditions showed, the average of the ears for almost all 4 samples was below 100nm, having decrease to a value near zero after 6 minutes. AFM measurements confirm the total planarization of lift-off ears, as can be seen from fig. 8. From the AFM image of lift-off ears (fig. 7), one can see the irregularity which characterizes this type of structure, not only in the direction of the metal's limit, but also vertically.

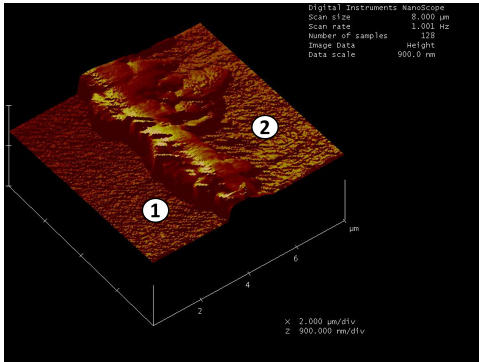


Figure 7: AFM image of lift-off ears before planarization.

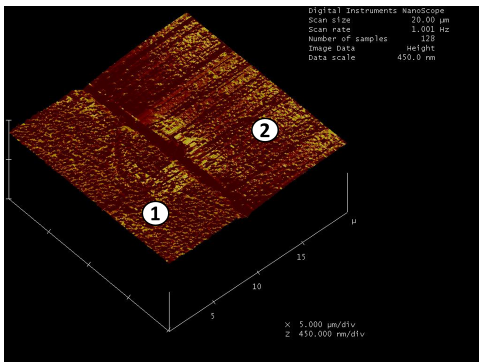


Figure 8: AFM image of lift-off ears after planarization.

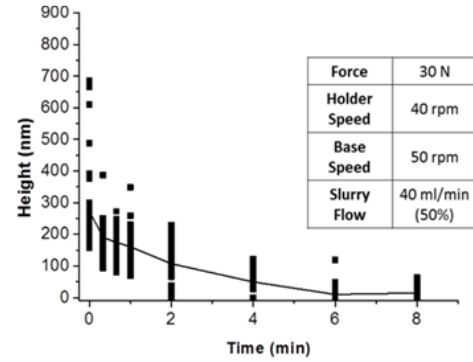


Figure 9: Lift-off ears planarization by CMP.

#### 3.2 Pillar access

For the pillar access, the topography of the oxide above the MTJ pillar and the Top Electrode, Bottom Electrode and Pillar (according to fig.4) were measured, with the results presented in fig.10. The Top Electrode and Bottom Electrode don't present a significant reduction of their height. On the other hand, the Pillar presents a significant decrease in height compared to the other two positions. The topography originated by the deposition of oxide above the pillar, tends to level with the Bottom Electrode as the polishing happens, presenting a much higher polishing rate for the pillar than to the Top or Bottom Electrode positions. The oxide above the pillar is planarizing in relation to the immediately surrounding area.

The polishing rates present in the graphics (numbers between each time step) also show another interesting result. The larger the difference between Pillar and Bottom Electrode, the larger the polishing rate. For example, between time=0min and time=2min, the height difference

between Pillar and Bottom Electrode is clearly larger for A2. The polishing rate for this sample is also higher than it is for sample A3. This result can be somewhat accepted in light of the fact that the polishing pad will act more aggressively in the most prominent features that it will on features that are about the same size, thus enhancing the mechanical effect of the CMP.

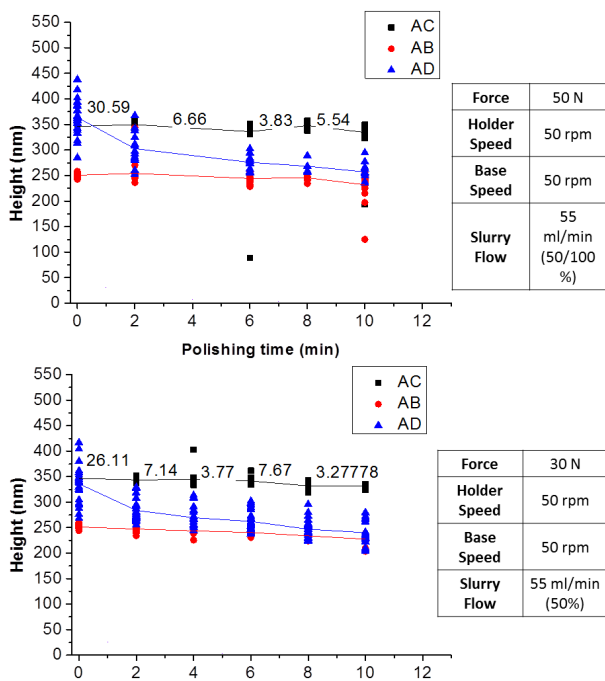


Figure 10: Height of the structures measured until contact is opened with the pads.

To study the effect of the polishing rate in different areas, polishing rates of sensors whose pillars had different areas were compared to each other and to the contact pad. The results don't show any particular tendency of polishing rate variation with the pillar area, although, the polishing rate of the pillars compared to the polishing rate of the contacts ('Pad') is much larger, in general.

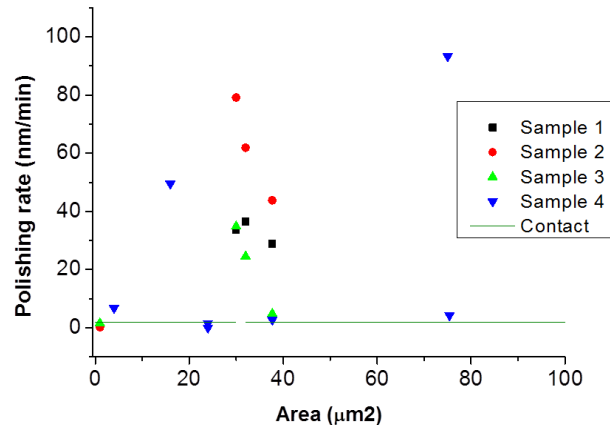


Figure 11: Polishing rate versus area of the base area of the pillar and the area of the contact pad.

### 3.3 MR measurements

To obtain a MR curve, the sample is placed in the middle of two Helmholtz coils which produce a magnetic field along the sample easy axis, varying between -140 Oe and 140 Oe. A current source (KEITHLEY 220 Programmable current source) feeds the MTJ sensor with a current, while a voltmeter reads the voltage (KEITHLEY 182 Sensitive Digital Voltmeter). These equipments are all controlled and their informations read through a GPIB bus connected to a computer by USB interface.

The MR response for most sensors in the sample was nonexistent. Each sample had 1020 sensors; 37 were measured, 24% of which presented a MR response. In fig. 12 is presented a MR response of a workign MTJ sensor.

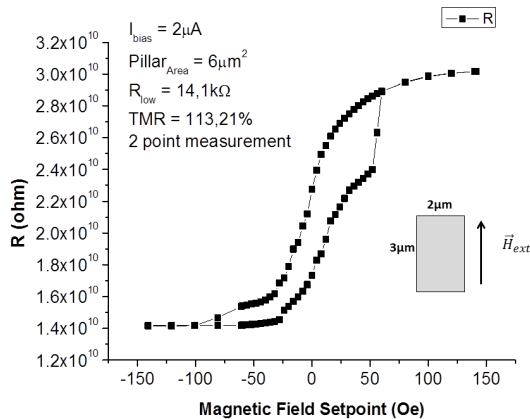


Figure 12: MR response for a MTJ sensor.

## 4 Conclusion

The fabrication of MR sensors using CMP was achieved, although with a very low yield. The faster polishing of the oxide above the pillars compared to the oxide above the contact pads may have compromised the integrity of the magnetic layers in the pillar, or, removed the oxide from the MTJ pillar's sides. In the first case, the MR response would be compromised since the magnetic layers have been damaged; in the second case, the current could short-circuit the barrier, since the metal deposition after the third lithography would be deposited around the pillar.

To improve the fabrication of MTJ sensors using CMP, a new approach should be chosen. The low yield presented could be improved by, after the pillar definition by etch, depositing immediately the oxide, without removing the photoresist. This could provide another protective layer against pol-

ishing, but since the oxide would be deposited with photoresist, after its removal undesired topography could also appear around the MTJ pillar.

Since the oxide on top the pillars is polished at a higher speed than the one on top of the contact pads, a good approach would be to define only the pillar in the second lithography, and not the contact pads, insulating after this the pillar. An extra lithography would then protect all surface except the one above the bottom contact metal and the unprotected oxide would be removed by etch.

For the removal of undesired topography, the use of CMP has proven a good technique, having reduced it to a height near 0nm after 6min.

## References

- [1] P. B. Zantye, A. Kumar, A. K. Sikder, *Chemical mechanical planarization for microelectronics applications*, Materials Science and Engineering, Vol. 45, 2004
- [2] Y. Nishi, R. Doering, *Handbook of Semiconductor Manufacturing Technology, Second Ed*, CRC Press, Taylor Francis Group, 2008.
- [3] Rita J. S. Macedo, *Spintronic Nano Devices: Nanofabrication of sub-50nm Magnetic Tunnel Junctions and Self-Powered Hybrid Sensors*, PhD Thesis, Instituto Superior Técnico, 2010.